# Highly Ordered Nanoporous Thin Films by Blending of PSt-*b*-PMMA Block Copolymers and PEO Additives as Structure Directing Agents

SUNG CHAN PARK,[1] HYUNJUNG JUNG,[1] KEN-ICHI FUKUKAWA,[2] LUIS M. CAMPOS,[2] KYUNGHEE LEE,[3] KYUSOON SHIN,[3] CRAIG J. HAWKER,[2] JEONG SOOK HA,[1] JOONA BANG[1]

[1]Department of Chemical and Biological Engineering, Korea University, Seoul 136-701, Republic of Korea

[2]Materials Research Laboratory, University of California, Santa Barbara, California 93106

[3]School of Chemical and Biological Engineering, Seoul National University, Seoul 151-744, Republic of Korea

*Received 13 September 2008; accepted 26 September 2008*
*DOI: 10.1002/pola.23102*
*Published online in Wiley InterScience (www.interscience.wiley.com).*

**ABSTRACT:** Herein, we present a simple method for producing nanoporous templates with a high degree of lateral ordering by self-assembly of block copolymers. A key feature of this approach is control of the orientation of polymeric microdomains through the use of hydrophilic additives as structure directing agents. Incorporation of hydrophilic poly(ethylene oxide) (PEO) moieties into poly(styrene-*b*-methyl methacrylate) (PSt-*b*-PMMA) diblock copolymers gives vertical alignment of PMMA cylinders on the substrate after solvent annealing. Because of the miscibility between PEO and PMMA, PEO additives were selectively positioned within PMMA microdomains and by controlling the processing conditions, it was found that ordering of PSt-*b*-PMMA diblock copolymers could be achieved. The perpendicular orientation of PMMA cylinders was achieved by increasing the molecular size of the PEO additives leading to an increased hydrophilicity of the PMMA domains and consequently to control the orientation of microdomains in PSt-*b*-PMMA block copolymer thin films. © 2008 Wiley Periodicals, Inc. J Polym Sci Part A: Polym Chem 46: 8041–8048, 2008
**Keywords:** additives; block copolymers; star polymers; thin films

## INTRODUCTION

Nanoporous thin films prepared by self-assembly of block copolymers have received significant attention due to the wide range of potential applications, such as microelectronics, data storage media, separation membranes, high surface area catalyst supports, biosensors, photovoltaic cells, etc. envisaged for these materials.[1–16] It is now well established that the structural characteristics of block copolymer thin films can be controlled by manipulation of molecular weight, block volume fraction, and the interaction parameter, $\chi$.[1,4,5] In turn the orientation of the block domains in thin films is governed by boundary conditions such as commensurability and interfacial interaction between blocks and substrates.[1,4,5] In controlling the orientation of block copolymers in thin films, several strategies have been employed including surface modification,[17–20] solvent annealing,[21] electric fields,[22] graphoepitaxy,[23] chemical prepatterning,[24,25] shear,[26] etc.

*Correspondence to:* C. J. Hawker (E-mail: hawker@mrl.ucsb.edu), J. S. Ha (E-mail: jeongsha@korea.ac.kr), or J. Bang (E-mail: joona@korea.ac.kr)

Journal of Polymer Science: Part A: Polymer Chemistry, Vol. 46, 8041–8048 (2008)

Among various block copolymer systems examined, poly(styrene-*b*-methyl methacrylate) (PSt-*b*-PMMA) diblock copolymers are widely studied for block copolymer lithography and the generation of highly ordered nanoporous templates due to the facile control of vertical alignment and use of standard semiconductor processing techniques, such as UV irradiation, for removal of the PMMA domains.[18] Traditionally, the orientation of PMMA microdomains has been controlled by manipulating the surface interaction using an ultrathin neutralization layer of PSt-*r*-PMMA random copolymers.[17–20] However, the major drawback of this system is the presence of grain boundaries and defect structures, which is not desirable for many applications that require registration, such as addressable storage media. To overcome these challenges, it has been demonstrated that simple solvent annealing of cylinder-forming poly(styrene-*b*-ethylene oxide) (PSt-*b*-PEO) block copolymer thin films can lead to a perpendicular orientation with a high degree of lateral ordering and no requirement for a neutralization layer.[21] Since the PEO block is not easily removed, cylinder-forming PSt-*b*-PMMA-*b*-PEO triblock copolymers that consist of PEO core and a cleavable PMMA shell have been developed[27] while Russell has also demonstrated the incorporation of cleavable functional groups at the PSt-*b*-PEO junction point.[28] In these cases, the PEO block provides good lateral ordering while the degradable units facilitate processing leading to highly ordered nanoporous templates.

In a similar manner to the PEO based block copolymers, PSt-*b*-PEO and PSt-*b*-PMMA-*b*-PEO, we previously showed that addition of hydrophilic PEO-coated gold nanoparticles, Au-PEO, to PSt-*b*-PMMA block copolymer can also lead to the highly ordered nanoporous thin films.[29] From this observation, it was suggested that the ordering mechanism in this system is similar to PEO-based copolymers where the PMMA-PEO blend mimics the behavior of the pure PEO systems. A key factor is the interaction between the hydrophilic components (PEO blocks or Au-PEO nanoparticles) and water vapor during the solvent annealing process.[29–31] In this work, we further analyze and simplify the use of surfactant-mediated self-assembly and examine other hydrophilic PEO additives, such as linear and star PEO, to examine the effect of molecular weight and chain architecture on the ordering of PSt-*b*-PMMA block copolymer thin films. This approach offers important advantages over the previous systems. First, nanoporous templates with good lateral ordering can be easily prepared by simply blending a small amount of PEO additives, which are readily available from commercial sources, with PSt-*b*-PMMA block copolymers. In addition, the linear and star PEO derivatives can be safely used as lithographic masks without disrupting the etching process, as there are no inorganic components, which is in stark contrast to the Au-PEO nanoparticles. Finally, the addition of small amounts of PEO additives can avoid any complications arising from complex morphologies that may occur in the case of ABC triblock copolymers.

## EXPERIMENTAL

### Materials

A cylinder-forming poly(styrene-*b*-methyl methacrylate) (PSt-*b*-PMMA) diblock copolymer with an overall molecular weight, $M_n$ of 140 kg/mol and a polydispersity of 1.06 was synthesized by living anionic polymerization. The block polymers were characterized by size exclusion chromatography (SEC) and by $^1$H, $^{13}$C NMR and IR spectroscopy. Linear PEO homopolymers with molecular weights $M_n$ of 4.0 and 10.0 kg/mol were purchased from Polymer source Inc., and are denoted EO-H4 and EO-H10, respectively. PEO star polymers with different number of arms and molecular weights were also used. As described in Table 1, the samples were designated EO-SX(Y), where X and Y denote the total molecular weight in kg/mol and the number of arms, respectively. The samples, EO-S2(4), EO-S7(8), and EO-S16(8), were purchased from Polymer source Inc., and EO-S100(20) was synthesized by living free-radical polymerization according to the literature.[32] EO-S100(20) has a poly(*N*,*N*-dimethylacrylamide) (PDMA) core and ~20 PEO arms. The total molecular weight and the number of arm for EO-S100(20) were estimated from SEC and $^1$H NMR, while those values for the other PEO star polymers were provided by the commercial source. The hydrodynamic diameters, $D_h$, of linear and star PEO were measured by dynamic light scattering (DLS) using a He-Ne ($\lambda$ = 636 nm) laser and BI-9000AT digital autocorrelator.

### Thin Film Preparation/Characterization

The thin films were prepared as following. PSt-*b*-PMMA diblock copolymers were dissolved in benzene, to which various amounts of PEO additives

**Table 1.** Characteristics of Linear and Star PEO Derivatives, in All Cases the PDI Was 1.20 or Less

| Sample I. D. | Type | Number of Arms | Mol. Wt. of Arms $M_n$ (g/mol) | Overall Mol. Wt., $M_n$ (g/mol) | Hydrodynamic Diameter (nm) |
|---|---|---|---|---|---|
| EO-H4 | Linear polymer | N/A | 4000 | 4000 | 2.8 |
| EO-H10 | Linear polymer | N/A | 10,000 | 10,000 | 3.8 |
| EO-S2(4) | Star polymer | 4 | 500 | 2000 | 1.4 |
| EO-S7(8) | Star polymer | 8 | 880 | 7800 | 6.0 |
| EO-S16(8) | Star polymer | 8 | 2000 | 16,000 | 8.1 |
| EO-S100(20) | Star copolymer | ~20 | 5000 | 120,000 | 15.2 |

were added. The total concentration of polymers was 1 wt %, and the amount of PEO additives relative to the block copolymers were adjusted from 0 to 10 wt %. Homogeneous solutions were then spin-coated onto silicon substrates with a native oxide layer, resulting in a film thickness ~40 nm. The films were transferred to a home-built glovebox chamber, and then annealed under saturated benzene environment and controlled humidity conditions, for at least 12 h. The detailed experimental set up and conditions for solvent annealing process have been described elsewhere.[29–31] The relative humidity (RH) within the chamber was maintained at ~90%. After solvent annealing, the film morphologies were characterized by scanning electron microscope (SEM) (Hitachi *S*-4300 SE) operating at 15 keV. The SEM images were obtained from nanoporous films, which were prepared by UV irradiation ($\lambda = 254$ nm), followed by rinsing with acetic acid and deionized water to remove the cylindrical microdomains (PMMA degradation products and PEO chains). To investigate the chemical composition of film surfaces (before UV irradiation), X-ray photoelectron spectroscopy (XPS) was performed at UCSB on a Kratos Axis Ultra Spectrometer (Kratos Analytical, Manchester, UK) using monochromated AlK$\alpha$ X-rays. The XPS spectra were collected at 70° emission angle (along the film surface).

## RESULTS AND DISCUSSION

In a previous study, three-dimensional, hydrophilic Au-PEO nanoparticles were used to direct the orientation of PSt-*b*-PMMA block copolymer thin films via solvent annealing after blending.[29] Because of the miscibility between PEO and PMMA, the Au-PEO nanoparticles were selectively positioned within the PMMA cylindrical microdomains. During solvent annealing under high humidity conditions (~90%), the preferential interaction of the PEO nanoparticles with water vapor induces the perpendicular orientation of PMMA microdomains. In this case, the effect of the Au-PEO nanoparticles could be due to either the three-dimensional, hard sphere nature of the nanoparticle or the hydrophilic nature of the PEO chains. To investigate this in greater detail, and aiming to identify simpler blend additives, a structure/property investigation of other hydrophilic PEO derivatives on the ordering of PSt-*b*-PMMA thin films was undertaken. In this regard, we employed PEO based macromolecules with various chain architectures, such as linear and star PEO, and explored the effect of these hydrophilic moieties on the ordering of PSt-*b*-PMMA thin films. As listed in Table 1, two linear PEO homopolymers, EO-H4 and EO-H10, and four PEO star polymers, EO-S2(4), EO-S7(8), EO-S16(8), and EO-S100(20), were blended with a PSt-*b*-PMMA diblock copolymer. The overall molecular weight, $M_n$ for the diblock copolymer was 140 kg/mol which leads to PMMA cylindrical microdomains, which have a pore diameter of 24 nm and periodicity of 67 nm.

As illustrated in Scheme 1, the PEO additives and PSt-*b*-PMMA block copolymer were mixed in benzene and spin coated onto silicon substrates. The relative amounts of PEO additives were varied from 0 to 10 wt % and the film thickness was maintained at ~40 nm for all samples which were subsequently annealed within a home-built

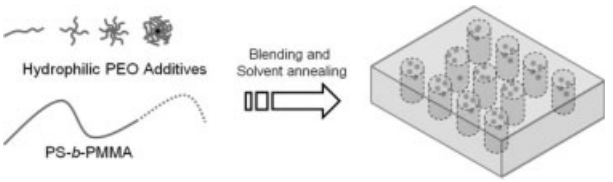


**Scheme 1.** Schematic representation of the blending and solvent annealing strategy for the preparation of PEO containing PSt-*b*-PMMA thin films that are vertically aligned under high humidity conditions.

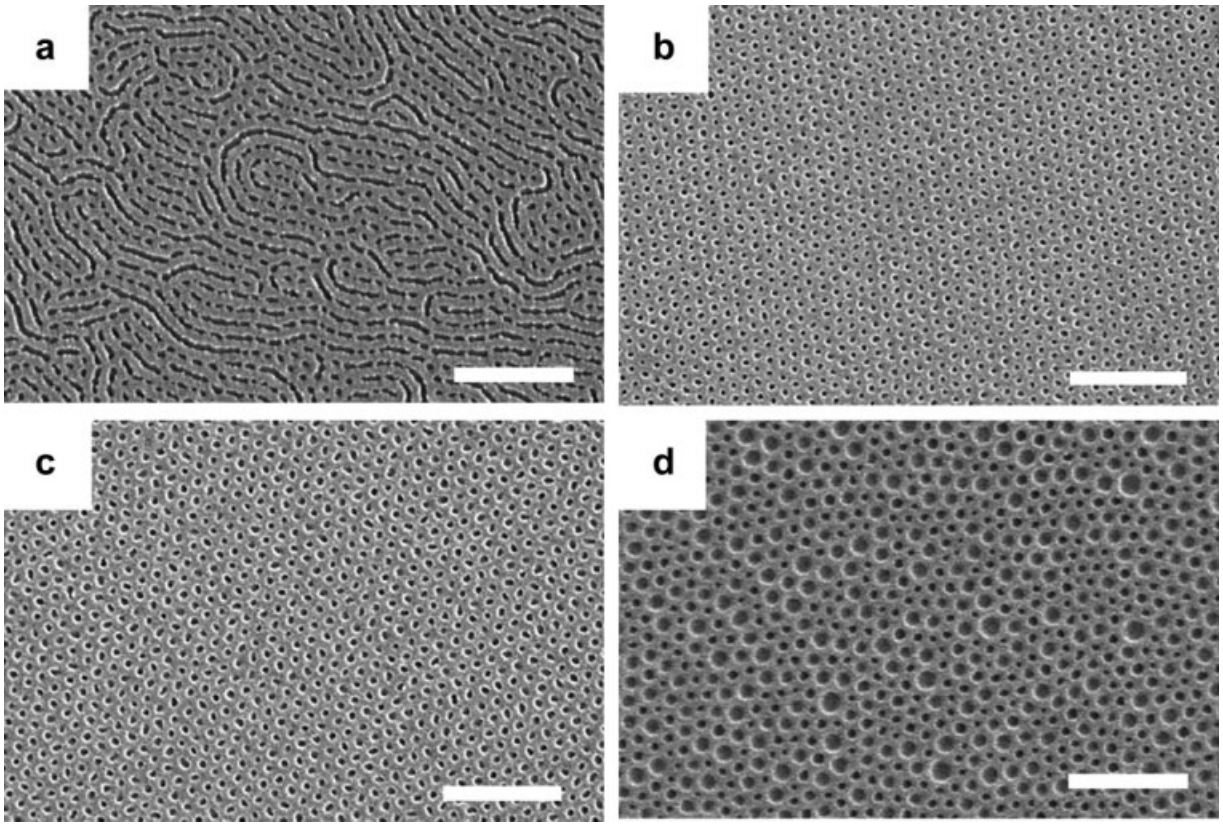


**Figure 1.** SEM images for PSt-*b*-PMMA thin films containing (a) 1.0 wt %, (b) 3.0 wt %, (c) 5.0 wt %, and (d) 10.0 wt % of EO-S100(20) after solvent annealing under high humidity conditions (~90%), followed by UV treatment and rinsing with acetic acid to remove PMMA microdomains. Scale bars are 500 nm.

glovebox chamber under a saturated benzene vapor and controlled relative humidity (RH) conditions. After solvent annealing, all films were exposed to UV light and then rinsed with acetic acid and water to remove the hydrophilic domains and to produce the nanoporous thin films. In addition to standard linear and star PEO derivatives, a core-shell PEO star copolymer was prepared using living free-radical polymerization to mimic the Au-PEO nanoparticles.[32] The resulting star copolymer, EO-S100(20), consists of a poly(*N,N*-dimethylacrylamide) (PDMA) core and PEO shell. The hydrodynamic diameter measured by DLS was 15.2 nm which is similar to the Au nanoparticles and within the size regime of the PMMA domains in the PSt-*b*-PMMA block copolymer.

Figure 1 represents the SEM images of nanoporous thin films formed by blending various amount of high molecular weight core-shell star copolymer, EO-S100(20) and annealing under high humidity conditions (~90%), followed by removal of cylindrical microdomains. The film morphologies were observed to be strongly dependent on the loading of the EO-S100(20) star copolymers. At 1.0 wt % addition of EO-S100(20), cylindrical microdomains are aligned parallel to the substrate, implying that interaction between hydrophilic particles and water vapor is not strong enough to induce perpendicular orientation of microdomains. In this case, the orientation can be directed by the preferential interaction between PMMA block and silicon substrate, and thus the parallel orientation is observed. With increasing amounts of EO-S100(20), 3.0 and 5.0 wt %, perpendicular orientation of cylindrical microdomains was achieved as is evidenced by highly-ordered hexagonal arrays of cylindrical pores [Fig. 1(b,c)]. It should also be noted that lateral ordering spans $\sim 2 \times 2\ \mu m^2$ area, which is characteristic for solvent annealed films of PEO based copolymer systems such as PSt-*b*-PEO and PSt-*b*-PMMA-*b*-PEO block copolymers.[21,27] Further increasing the amount of star copolymer to 10.0 wt % led to arrays of cylindrical pores.

However, lateral ordering is significantly disrupted due to the irregular pore size, which can be attributed to macrophase separation of the PEO star copolymers due to the high loading of hydrophilic nanoparticles added in the blend with the PSt-*b*-PMMA diblock copolymer.[29] From these results it can be concluded that the overall thin film behavior is similar for blends with both the Au-PEO nanoparticles and PEO star copolymers, demonstrating that the hard inorganic core is not necessary for efficient structure direction.

Based on the success with the PEO star copolymers, it was a natural extension to examine other PEO-based hydrophilic additives and determine if simpler structures can behave similarly by inducing orientational order of PSt-*b*-PMMA thin films. In these studies, commercially available PEO based linear and star polymers with different molecular weights and chain architectures, as listed in Table 1, were examined. Compared to the EO-S100(20) star copolymer, the hydrodynamic diameters and molecular weights for EO-S2(4), EO-S7(8), and EO-S16(8) were significantly smaller (see Table 1). Figure 2(a–c) show the SEM images of nanoporous films containing 5 wt % of EO-S2(4), EO-S7(8), and EO-S16(8), respectively, after solvent annealing under high humidity conditions followed by removal of PMMA domains. When the smallest star polymer, EO-S2(4) $M_n$ = 2000 g/mol, was added to the PSt-*b*-PMMA block copolymer, perpendicular orientation of microdomains was not achieved and parallel cylinders similar to the pure diblock copolymer orientation on native silicon oxide was observed. However, with increasing the number of arms and the molecular weight of both the PEO arms and overall molecular weight, it was found that the microdomains were oriented perpendicular to the substrate with a high degree of lateral ordering [Fig. 2(b,c)]. In this case, the film morphologies upon adding various amounts of EO-S7(8) or EO-S16(8), from 1 to 10 wt %, were similar to Figure 1. In contrast, addition of linear PEO (5 wt % of EO-H4 or EO-H10) did not induce vertical orientation and as shown in Figure 3 and only parallel PMMA microdomains similar to the starting pure diblock was observed.

From these results, it is noticeable that the orientation of microdomains in this system is greatly affected by the architecture and molecular weight of the PEO additives. Higher molecular weight, branched PEO additives were observed to be more effective in directing the orientation of microdomains in PSt-*b*-PMMA thin films. This behavior can be understood by considering our hypothesis on the ordering mechanism. Previously, it was suggested that the ordering of PEO based copolymer systems is induced by the interaction of the hydrophilic PEO block with water vapor during the solvent annealing process.[29–31] Initially, the thin films are swollen with benzene and upon exposing the films to a controlled humidity atmosphere, the solvent in the film rapidly evaporates from the surface and the film surface undergoes cooling. Water vapor from the humid atmosphere then condenses on the cold surface

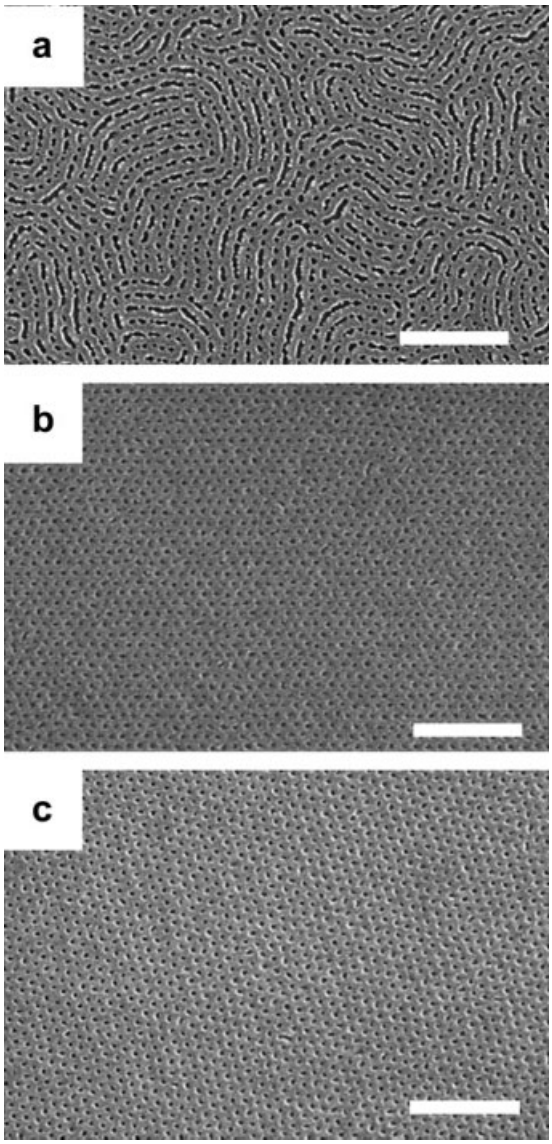


**Figure 2.** SEM images for PSt-*b*-PMMA thin films containing 5.0 wt % of PEO star polymers, (a) EO-S2(4), (b) EO-S7(8), and (c) EO-S16(8). All experimental conditions are same as Figure 1. Scale bars are 500 nm.

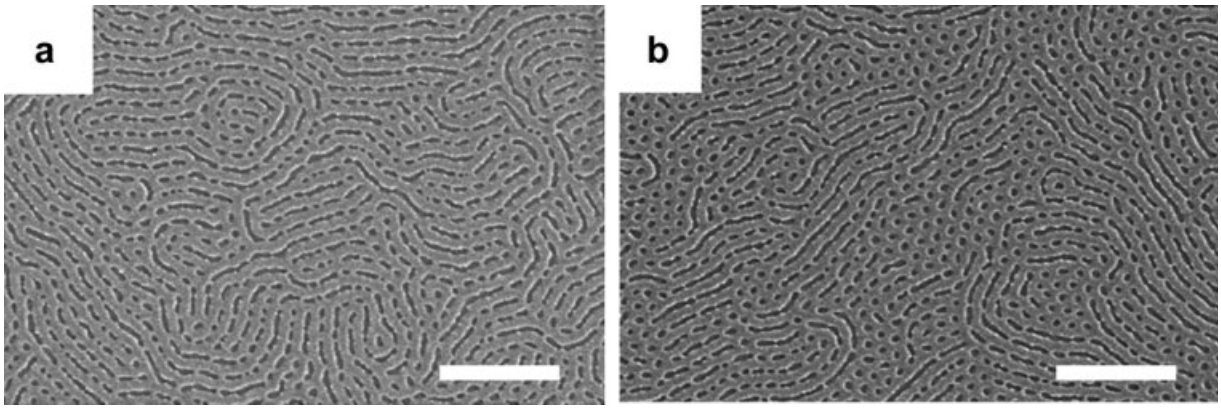


**Figure 3.** SEM images for PSt-*b*-PMMA thin films containing 5.0 wt % of linear PEO homopolymers, (a) EO-H4 and (b) EO-H10. All experimental conditions are same as Figure 1. Scale bars are 500 nm.

and interacts with the hydrophilic PEO domains. With further evaporation of solvent, the microdomains containing PEO undergo phase separation and at the air interface and propagate vertically down, leading to the perpendicular orientation of cylindrical microdomains. In this process, the most critical step for ordering is the interaction between water vapor and hydrophilic PEO-containing domains with the blending of hydrophilic PEO chains, while the PMMA domains undergo a similar interaction with water vapor to induce the perpendicular orientation of cylindrical microdomains. In this case, the results in Figures 2 and 3 suggest that high molecular weight, branched PEO derivatives lead to good structural templating performance. It can be conjectured that the larger hydrophilic PEO nanostructures are advantageous for nucleation (or condensation) of water vapor and consequently, templating the perpendicular orientation of the PMMA-PEO blended microdomains. As the size of PEO moieties increases, the miscibility with PMMA decreases, which can also facilitate the interaction with water vapor.

Based on the proposed ordering mechanism, it may be expected that a preferential segregation of PEO chains to the top surface of the film occurs during the solvent annealing process. To examine the presence of PEO chains at the surface of PSt-*b*-PMMA films, high resolution XPS was performed at the C 1s ionization edge with a 70° emission angle. Figure 4 shows a high resolution XPS spectra and its C 1s curve fitting of PSt-*b*-PMMA thin film containing 5.0 wt % of EO-S16(8) star copolymers after solvent annealing and perpendicular orientation of cylindrical microdomains. The three larger peaks at 284.8, 285.2, and 285.7 eV are due to the C-C bonds in PSt and PMMA with two small but distinct peaks present at 286.8 and 289.1 eV, which are due to the presence of C—O—C and O=C—O groups, respectively. Comparing both peak areas, it was found that the C—O—C peak is 140% larger than the O=C—O peak. Since the area of both peaks should be same for PMMA, the additional increment in the C—O—C peak can be attributed to the contribution from PEO. Therefore, it can be deduced that a significant amount of PEO chains are present at the top surface of the PSt-*b*-PMMA films.

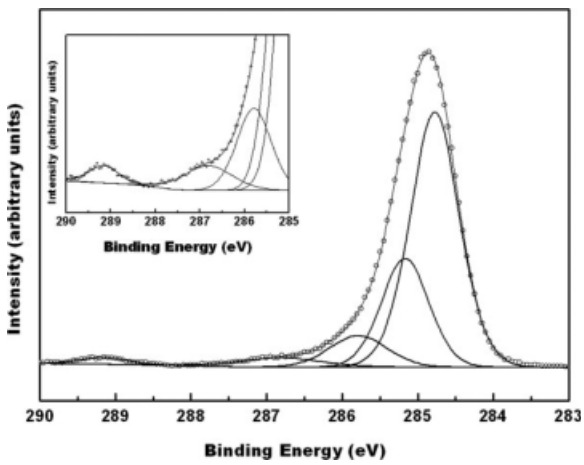


**Figure 4.** High resolution XPS spectra for PSt-*b*-PMMA thin films containing 5.0 wt % of EO-S16(8) after solvent annealing under high humidity conditions (~90%).

## CONCLUSIONS

In summary, nanoporous thin films have been prepared by blending of hydrophilic PEO additives and PSt-*b*-PMMA block copolymers. A variety of PEO molecular weights and chain architectures, such as linear and star PEO, were employed and the amounts blended with the PSt-*b*-PMMA block copolymer were controlled so that the overall cylindrical morphology of PSt-*b*-PMMA was not disturbed. The critical step in the ordering of PSt-*b*-PMMA thin films is the interaction between hydrophilic PEO moieties within the PMMA domains and water vapor under the high humidity conditions. In the absence of PEO additives, parallel orientation of the PMMA domains is observed. However, blending with PEO at low weight percentages (~5%) showed a dramatic change in nanostructures with orientation of PMMA cylinders normal to the substrate. It was found that the perpendicular orientation of microdomains was accompanied by a high degree of lateral ordering when high molecular weight, branched PEO derivatives were used. Low molecular weight and linear PEO macromolecules did not show any change in morphology when compared to the diblock copolymer. This strategy provides a simple and robust way to prepare nanoporous thin films without surface neutralization requirements and, furthermore, a new route to fabricate the functional templates with desired functional components.

This work was supported by Korean Science and Engineering Foundation (KOSEF) grants funded by the Korea government (MOST) (No. ROA-2007-000-20,102-0, M105030001 87-05M0300-18,710) and the UCSB Materials Research Laboratory (NSF Grant DMR05-20,415). S. C. Park appreciates a Seoul Science Fellowship. L. M. C. thanks the UC Regents for a UC President's Fellowship.

## REFERENCES AND NOTES

1. Hawker, C. J.; Russell, T. P. MRS Bull 2005, 30, 952–966.
2. Bita, I.; Yang, J. K. W.; Jung, Y. S.; Ross, C. A.; Thomas, E. L.; Berggren, K. K. Science 2008, 321, 939–943.
3. Ruiz, R.; Kang, H. M.; Detcheverry, F. A.; Dobisz, E.; Kercher, D. S.; Albrecht, T. R.; de Pablo, J. J.; Nealey, P. F. Science 2008, 321, 936–939.
4. Fasolka, M. J.; Mayes, A. M. Ann Rev Mater Res 2001, 31, 323–355.
5. Segalman, R. A. Mater Sci Eng R 2005, 48, 191–226.
6. Park, M.; Harrison, C.; Chaikin, P. M.; Register, R. A.; Adamson, D. H. Science 1997, 276, 1401–1404.
7. Black, C. T.; Guarini, K. W.; Zhang, Y.; Kim, H. J.; Benedict, J.; Sikorski, E.; Babich, I. V.; Milkove, K. R. IEEE Electron Device Lett 2004, 25, 622–624.
8. Black, C. T.; Ruiz, R.; Breyta, G.; Cheng, J. Y.; Colburn, M. E.; Guarini, K. W.; Kim, H. C.; Zhang, Y. IBM J Res Dev 2007, 51, 605–633.
9. Shin, K.; Leach, K. A.; Goldbach, J. T.; Kim, D. H.; Jho, J. Y.; Tuominen, M.; Hawker, C. J.; Russell, T. P. Nano Lett 2002, 2, 933–936.
10. Yang, S. Y.; Ryu, I.; Kim, H. Y.; Kim, J. K.; Jang, S. K.; Russell, T. P. Adv Mater 2006, 18, 709–712.
11. Lee, J. I.; Cho, S. H.; Park, S. M.; Kim, J. K.; Kim, J. K.; Yu, J. W.; Kim, Y. C.; Russell, T. P. Nano Lett 2008, 8, 2315–2320.
12. Demirel, A. L.; Yurteri, S.; Cianga, I.; Yagci, Y. J Polym Sci Part A: Polym Chem 2007, 45, 2091–2104.
13. Forcen, P.; Oriol, L.; Sanchez, C.; Alcala, R.; Hvilsted, S.; Jankova, K.; Loos, J. J Polym Sci Part A: Polym Chem 2007, 45, 1899–1910.
14. Fustin, C. A.; Guillet, P.; Misner, M. J.; Russell, T. P.; Schubert, U. S.; Gohy, J. F. J Polym Sci Part A: Polym Chem 2008, 46, 4719–4724.
15. Jin, M.; Lu, R.; Yang, Q. X.; Bao, C. Y.; Sheng, R.; Xu, T. H.; Zhao, Y. Y. J Polym Sci Part A: Polym Chem 2007, 45, 3460–3472.
16. Sandholzer, M.; Bichler, S.; Stelzer, F.; Slugovc, C. J Polym Sci Part A: Polym Chem 2008, 46, 2402–2413.
17. Mansky, P.; Liu, Y.; Huang, E.; Russell, T. P.; Hawker, C. J. Science 1997, 275, 1458–1460.
18. Thurn-Albrecht, T.; Steiner, R.; DeRouchey, J; Stafford, C. M.; Huang, E.; Bal, M.; Tuominen, M.; Hawker, C. J.; Russell, T. P. Adv Mater 2000, 12, 787–790.
19. Ryu, D. Y.; Shin, K.; Drockenmuller, E.; Hawker, C. J.; Russell, T. P. Science 2005, 308, 236–239.
20. Bang, J.; Bae, J.; Lowenhielm, P.; Spiessberger, C.; Given-Beck, S. A.; Russell, T. P.; Hawker, C. J. Adv Mater 2007, 19, 4552–4557.
21. Kim, S. H.; Misner, M. J.; Xu, T.; Kimura, M.; Russell, T. P. Adv Mater 2004, 16, 226–231.
22. Thurn-Albrecht, T.; DeRouchey, J.; Russell, T. P.; Kolb, R. Macromolecules 2002, 35, 8106–8110.
23. Segalman, R. A.; Yokoyama, H.; Kramer, E. J. Adv Mater 2001, 13, 1152–1155.
24. Kim, S. O.; Solak, H. H.; Stoykovich, M. P.; Ferrier, N. J.; de Pablo, J. J.; Nealey, P. F. Nature 2003, 424, 411–414.
25. Stoykovich, M. P.; Mueller, M.; Kim, S. O.; Solak, H. H.; Edwards, E. W.; de Pablo, J. J.; Nealey, P. F. Science 2005, 308, 1442–1446.

26. Angelescu, D. E.; Waller, J. H.; Adamson, D. H.; Deshpande, P.; Chou, S. Y.; Register, R. A.; Chaikin, P. M. Adv Mater 2004, 16, 1736–1740.
27. Bang, J.; Kim, S. H.; Drockenmuller, E.; Misner, M. J.; Russell, T. P.; Hawker, C. J. J Am Chem Soc 2006, 128, 7622–7629.
28. Zhang, M.; Yang, L.; Yurt, S.; Misner, M. J.; Chen, J.-T.; Coughlin, E. B.; Venkataraman, D.; Russell, T. P. Adv Mater 2007, 19, 1571–1576.
29. Park, S. C.; Kim, B. J.; Hawker, C. J.; Kramer, E. J.; Bang, J.; Ha, J. S. Macromolecules 2007, 40, 8119–8124.
30. Bang, J.; Kim, B. J.; Stein, G. E.; Russell, T. P.; Li, X.; Wang, J.; Kramer, E. J.; Hawker, C. J. Macromolecules 2007, 40, 7019–7025.
31. Tang, C.; Bang, J.; Stein, G. E.; Fredrickson, G. H.; Hawker, C. J.; Kramer, E. J.; Sprung, M.; Wang, J. Macromolecules 2008, 41, 4328–4339.
32. Fukukawa, K. I.; Rossin, R.; Hagooly, A.; Pressly, E. D.; Hunt, J. N.; Messmore, B. W.; Wooley, K. L.; Welch, M. J.; Hawker, C. J. Biomacromolecules 2008, 9, 1329–1339.